

HOSTED BY



Contents lists available at ScienceDirect

Saudi Pharmaceutical Journal

journal homepage: www.sciencedirect.com

Original article

A cheminformatics-biophysics correlate to identify promising lead molecules against matrix metalloproteinase-2 (MMP-2) enzyme: A promising anti-cancer target

Faris Alrumaihi

Department of Medical Laboratories, College of Applied Medical Sciences, Qassim University, Buraydah 51452, Saudi Arabia

ARTICLE INFO

Article history:

Received 8 April 2023

Accepted 10 May 2023

Available online 16 May 2023

Keywords:

Matrix metalloproteinase-2

CMNPD8322

CMNPD8320

CMNPD8318

Molecular dynamic simulation

WaterSwap

ABSTRACT

Matrix metalloproteinase-2 (MMP-2) is an endopeptidase enzyme that is devoted to extracellular matrix proteins degradation. The enzyme is warranted as promising drugs target for different light threatening diseases such as arthritis, cancer and fibrosis. Herein, in this study, three drug molecules: CMNPD8322, CMNPD8320, and CMNPD8318 were filtered as high affinity binding compounds with binding energy score of -9.75 kcal/mol, -9.11 kcal/mol, -9.05 kcal/mol, respectively. The control binding energy score was -9.01 kcal/mol. The compounds docked deeply inside the pocket interacting with S1 pocket residues. The docked complexes dynamics in real time at cellular environment was then done to decipher the stable binding conformation and intermolecular interactions network. The compounds complexes achieved very stable dynamics with root mean square deviation (RMSD) with mean value of around $2-3$ Å compared to control complex that showed higher fluctuations of 5 Å. The simulation trajectories frames based binding free energy demonstrated all the compounds-MMP-2 complexes reported highly stable energy, particularly the van der Waals energy dominate the overall net energy. Similarly, the complexes revalidation of WaterSwap based energies also disclosed the complexes highly stable in term docked conformation. Also, the compounds illustrated the compounds favorable pharmacokinetics and were non-toxic and non-mutagenic. Thus, the compounds might be used thorough experimental assays to confirm compounds selective biological potency against MMP-2 enzyme.

© 2023 The Author(s). Published by Elsevier B.V. on behalf of King Saud University. This is an open access article under the CC BY-NC-ND license (<http://creativecommons.org/licenses/by-nc-nd/4.0/>).

1. Introduction

Matrix Metalloproteinase-2 (MMP-2) enzyme is devoted to extracellular matrix components degradation and play a critical role migration of breast cancer, gastric, prostate, and pancreatic cancer cells (Jeziarska and Motyl, 2009). The enzyme is 72 kDa biomolecule and is encoded by MMP2 gene present on chromosome 16 at position 12.2 (Tauro and Lynch, 2018). The major implication of MMP-2 in cancer progression is to activate metastases (Bodnar et al., 2015; Hung et al., 2021). Particularly, the MMP-2 together with MMP-9 is capable of type IV collagen degradation (Hernandez-Guillamon et al., 2015; Kurzepa et al., 2014). The basement membrane is key to maintaining tissue organization thus

providing structural support to cells and affecting cell polarity and signaling (Dvorak et al., 2011). This degradation of basement membrane is necessary step in most cancer metastatic progression (Banerjee et al., 2022; Benton et al., 2011).

Several MMP-2 inhibitors have been proposed in clinical trials showing promising results (Webb et al., 2017; Zhong et al., 2018). According to phase I clinical trials, the MMP inhibitors were disclosed generally safe with less adverse effects. It is also reported that in clinical trials marimastat show improved patient survival suffering from pancreatic and gastric cancer (Winer et al., 2018). Different research groups proposed many strategies in effective MMP inhibitors designing for cancer treatment. Among these, the first and vital approach is to target specific MMP function thus allowing doctors to increase treatment dosage while keeping the side effects to minimum (Vandenbroucke and Libert, 2014). Another approach could be to administer specific MMP inhibitors together with proteinase or cytotoxic agents (Vandooren et al., 2016). The third approach is to use MMP inhibitors in early cancer stages to block cancer invasion and metastasis (Brown and Murray, 2015). In another approach, the tumor overexpression of MMP can be utilized as potential target for release of chemotherapeutic

E-mail address: f_alrumaihi@qu.edu.sa

Peer review under responsibility of King Saud University.



Production and hosting by Elsevier

<https://doi.org/10.1016/j.jsps.2023.05.010>

1319-0164/© 2023 The Author(s). Published by Elsevier B.V. on behalf of King Saud University.

This is an open access article under the CC BY-NC-ND license (<http://creativecommons.org/licenses/by-nc-nd/4.0/>).

agents at specific tumor sites (Barve et al., 2014). The siRNA or cytotoxic agents may also be encapsulated in viral vectors or liposomes that can be cleaved by target MMP and activate the agents (Khan et al., 2021). Other way of MMP inhibition is by coupling MMP inhibitors with imaging agents that aid in tumors detection before it spread (Kessenbrock et al., 2010).

Targeting MMP-2 by small inhibitors is an attractive way to block the enzyme function. Compared to conventional drug discovery, computer aided drug design or CADD contributed significantly to modern drug discovery (Muhseen et al., 2020; Noor et al., n.d.; Tahir ul Qamar et al., 2020). The CADD is a broad term comprising vast computational and theoretical approaches helping in drugs discovery and optimization against any given biomolecule (Hassan Baig et al., 2016). The CADD techniques have emerged and evolved in perspective of experimental approaches. The main goal of the CADD is to identify/develop potential lead structures (Ahmad et al., 2018; Alamri et al., 2023; Shaker et al., 2021). The CADD approaches are gaining much popularity in recent years both in pharmaceutical industries and academia. These methods are cost effective, fast and importantly save time by shortening the drug discovery time line (L Mallipeddi et al., 2014). Herein, in this work, a multi-pronged computational approach was applied with main goal to identify compounds that bind best to the MMP-3 catalytic domain. The study comprises structure based virtual screening, molecular dynamic simulation, binding free energies and pharmacokinetic properties investigation (Ahmad et al., 2021; Altharawi et al., 2021; Lombardo et al., 2017; Maia et al., 2020; Singh et al., 2018; Wang et al., 2019). The prioritized lead molecules identified herein were subjected to all atoms dynamic environment in order to ensure real cellular intermolecular stability of docked complexes. Further, the intermolecular binding energies were estimated to get overall dominant energies that contributed significantly to lead molecules affinities for the MMP-2 enzyme. The study outcomes might of interest for experimentalists and may speed up drug discovery against cancer.

2. Materials and methods

The complete flow of methods used herein is described in Fig. 1.

2.1. MMP2 structure building

The X-ray diffraction determined crystal structure of human MMP-2 catalytic domain was accessed from RCSB protein database (Sussman et al., 1998). The four-digit code used for this purpose was “7XGJ”(Takeuchi et al., 2022). The MMP-2 protein domain structure was determined in *Escherichia coli* BL21 expression system at resolution of 2.80 Å and R-value observed of 0.227. The PDB contains inhibitor molecule of aryloxyphenyl-heptapeptide hybrid. The enzyme structure was then subjected to protein preparation wizard in UCSF Chimera v1.16 to remove co-crystallized ligand molecules and energy minimized the receptor molecule (Kaliappan and Bombay, 2018). The energy minimization was carried out using steepest descent algorithm for 1500 rounds with step size of 0.2 Å. This was followed by conjugate gradient algorithm for 2500 cycles with same step size value of 0.2 Å. The charge assignment was done via Gasteiger charge method. Once MMP2 structure building was done, the protein was saved in.pdb format.

2.2. Ligand library preparation

For virtual screening process, the comprehensive marine natural products database (CMNPD) was used (Lyu et al., 2021). The CMNPD is an open access knowledge database curated manually to accommodate compounds from marine sources. The CMNPD database is an excellent starting resource for screening diverse

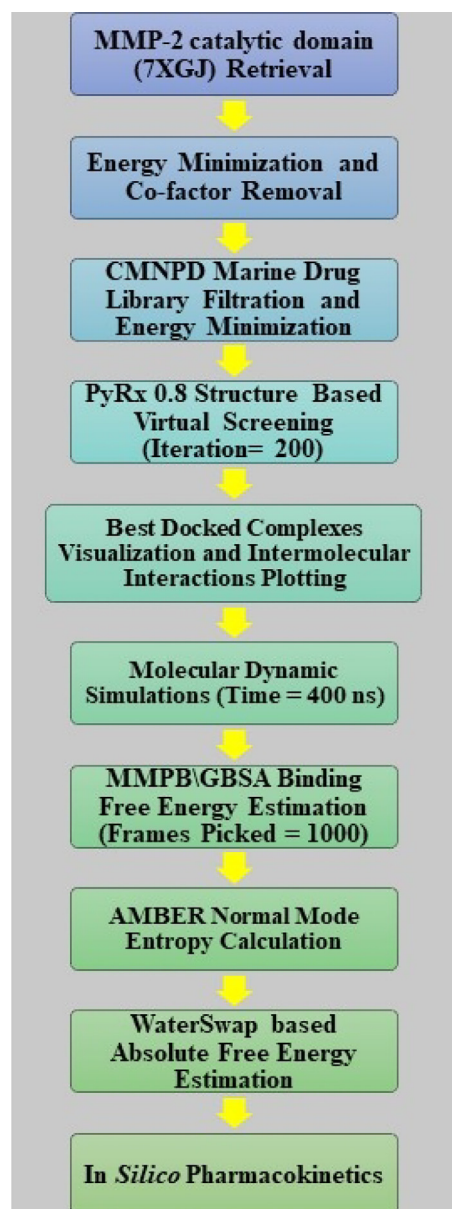


Fig. 1. The complete flow of work done in this study. The study was initiated by retrieving MMP-2 catalytic domain. The protein was then subjected to several different computer aided drug design methods in order to prioritize and understand intermolecular conformation and interactions network.

chemical structures against any given biological macromolecules and identify the best binding molecules. The CMNPD database comprised 47,451 compounds collected from marine bacteria, fungi, green algae, brown algae, red algae, and sponges. The database was retrieved in.sdf format and imported to LigandScout software where it was filtered based on Lipinski rule of five (Lipinski, 2004; Wolber and Langer, 2005). The Lipinski rule of five is a famous rule to filter only druglike molecules as they have high success chances to be marketed. After filtration, the filtered druglike molecules were then used in PyRx 0.8 for energy minimization and conversion to.pdbqt format (Dallakyan and Olson, 2015).

2.3. PyRx virtual screening

The CMNPD druglike molecules were then virtually screened against the MMP-2 catalytic domain in PyRx 0.8 software. The grid

box was set around His125:NE2 (x-axis = 23.393 Å, y-axis = -21.2 25 Å and z-axis = 2.685 Å), His131:NE2 (x-axis = 26.757 Å, y-axis = -21.457 Å and z-axis = 3.076 Å) and His121:NE2 (x-axis = 24.90 2 Å, y-axis = -18.616 Å and z-axis = 1.592 Å). The dimensions of the grid box were 25 Å on XYZ planes. The docking run for each compound to the receptor was 200. For comparative analysis, a control molecule (6-(10,13-dimethyl-3,6,15,16-tetraoxo-2,3,6,7,10,11,12,13,14,15,16,17-dodecahydro-1H-cyclopenta[a]phenanthren-17-yl)-2-methylheptanal) which is co-crystallized with the MMP-2 was employed. The inhibitory potential of the control compound is $IC_{50} = 0.20$ nM (Takeuchi et al., 2022). The best docked conformation was assigned with lowest binding energy score and thus complexed with MMP-2. The docked complexes were visualized in UCSF Chimera 1.16 (Kaliappan and Bombay, 2018) and Discovery Studio v2021 (Biovia, 2017).

2.4. Molecular dynamic simulation setup and production

The molecular dynamic simulation setup and production run were conducted using AMBER20 software (Ahmad et al., 2019a; Case et al., 2020; Ullah et al., 2021). The FF14SB force field was employed to model the receptor MMP2 structure parameters while compounds structure was treated with GAFF force field (Maier et al., 2015; Sprenger et al., 2015). The selected MMP2-compounds complexes were placed into TIP3P water box considering buffer distance of 12 Å (Ahmad et al., 2017). To counter systems charges, appropriate number of counter ions were added to the box. The simulation protocol was adopted from previous works. Each system was energy minimized for restraint of solute heavy atoms, energy minimization with no restraints, gradual heating of systems from 0 to 300 K, simulation under NPT ensemble at 1 bar pressure and temperature of 300 K, NPT ensemble simulation with solvent equilibration, protein heavy atoms simulation annealing from 10 to 2 kcal/mol, simulation of carbon alpha atoms at 2 kcal/mol, and production run of 400 ns (Abro and Azam, 2016). The SHAKE algorithm was used to apply constrain on bonds having hydrogen atoms (Kräutler et al., 2001). The long range electrostatic interactions were dealt with particle mesh Ewald method under periodic boundary conditions (Petersen, 1995). The simulation trajectories were evaluated for complexes structure deviations using AMBER CPPTRAJ module (Roe and Cheatham III, 2013). The simulation plots were created via XMGRACE v5.1 (Turner, 2005).

2.5. Estimating binding free energies

The Poisson–Boltzmann or generalized Born and surface area continuum solvation (MM/PBSA and MM/GBSA) methods were applied on the simulation trajectories to sample frames from regular time gap to investigate complexes intermolecular binding free energies (Ahmad et al., 2019a; Miller et al., 2012; Sahakyan, 2021). To accomplish this task, the MMPBSA.py module of AMBER was loaded to determine the net binding energy value, which is done via the following mathematical equation.

$$\Delta G_{\text{binding}} = G_{\text{complex}} - (G_{\text{protein}} + G_{\text{ligand}})$$

where $G = E_{\text{mm}} + G_{\text{SGB}} + G_{\text{NP}}$.

In the equation, G is the total binding energy composed of molecular mechanic's energy, G_{SGB} is solvation mode for estimating polar solvation and G_{NP} is nonpolar solvation energy. During the analysis, total of 1000 frames were used for net binding energy estimation. The entropy energy of each complex was calculated using AMBER normal mode entropy method (Genheden et al., 2012)a.

2.6. WaterSwap investigation

The WaterSwap calculation was done to revalidate the MMPB \GBSA binding free energy of complexes (Woods et al., 2014). The method is more sophisticated and reliable in order to surface the contribution of water molecules that play role in bridging ligand with MMP-2 catalytic domain residues (Woods et al., 2014, 2011). The docked complexes were energy minimized. For treating the compound, the GAFF version was used with AM1-BCC charge method. The solvation box size was kept to 10 Å. The energy minimization tolerance was set as 0.25 kcal/mol, followed by systems equilibration for 500 ps. The number of WaterSwap iterations used were 1000, which is considered enough for convergence of three algorithms such as free energy perturbation (FEP), thermodynamic integration (TI) and Bennett's (Ahmad et al., 2019b).

2.7. Radial distribution function (RDF) analysis

To delineate the critical intermolecular interactions and highlight their density distribution along the simulation time, RDF analysis was conducted (Abbasi et al., 2016; Donohue, 1954). The RDF input script was acquired from AMBER online platform and run via CPPTRAJ module. RDF plots were generated through XMGRACE v5.1 to quantify chemical interactions between receptor active pocket residue atoms with ligand atoms present in the pocket vicinity.

2.8. Computational pharmacokinetic prediction

The computational pharmacokinetic of filtered lead molecules was done via SwissADME (Daina et al., 2017) and pkCSM (Pires et al., 2015) online servers.

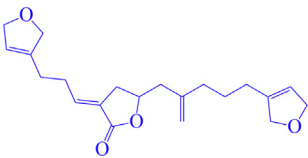
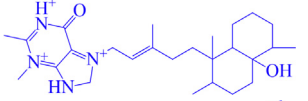
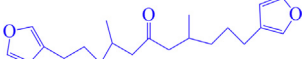
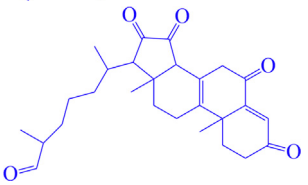
3. Results and discussion

3.1. Docking studies

The virtual screening process was conducted in order to determine the compounds that bind best to the MMP-2 enzyme. During structure based virtual screening process, several compounds were shortlisted the showed stable binding conformation at the catalytic domain of MMP-2 enzyme and score excellent in term of least binding energy in kcal/mol. Control molecule was used as define threshold value for best compounds selection. By doing so, three drug molecules were prioritized such as CMNPD8322, CMNPD8320, and CMNPD8318 as high affinity binding compounds with binding energy score of -9.75 kcal/mol, -9.11 kcal/mol, -9.05 kcal/mol, respectively. The control binding energy score was -9.01 kcal/mol. Table 1 list the lead compounds/control binding energy score and key hydrophilic and hydrophobic interactions. The CMNPD8322 is isonitenin and obtained from marine *Spongia (Spongia) officinalis*. The CMNPD8320 is purino-diterpene and is sourced from marine sponge *Agelas mauritiana*. Similarly, the CMNPD8318 is nakamurol C and is extracted from *Agelas nakamura*. The CMNPD8322 compound is (E)-5-(5-(2,5-dihydro furan-3-yl)-2-methylenepentyl)-3-(3-(2,5-dihydrofuran-3-yl)propylidene)dihydrofuran-2(3H)-one where as CMNPD8320, and CMNPD8318 is (E)-7-(5-(4a-hydroxy-1,2,5,5-tetramethyldecahydronaphthalen-1-yl)-3-methylpent-2-en-1-yl)-2,3-dimethyl-6-oxo-8,9-dihydro-6H-purine-1,3,7-trium and 1,11-di(furan-3-yl)-4,8-dimethylundecan-6-one, respectively. All the three compounds and the control was found to interact at the same pocket. In case of CMNPD8322, main contributions were seen from the central chemical moiety 5-methyl-3-methylenedihydrofuran-2(3H)-one formed two hydrogen bonds with Leu83 and Ala84 with bond dis-

Table 1

Selected three compounds and control along with binding energy, and residues involved in hydrogen bondings and hydrophobic interactions.

Compound	2D structure	Binding Energy in kcal/mol	Hydrogen bonds	Hydrophobic interactions
CMNPD8322		−9.75	Leu83, Ala84	Asp80, Gly81, Leu82, Tyr113, Leu117, Val118, His121, Ala137, Leu138, Ala140, Pro141, Ile142, Tyr143, Tyr144, Phe149,
CMNPD8320		−9.11	Gly81, Ala140, Ile142	Leu82, Ala84, Leu117, Val118, His121, His131, Ala137, Leu138, Pro141, Tyr143, Thr144, Phe149
CMNPD8318		−9.05	Gly81	Asp80, Leu82, Leu83, Ala84, Tyr113, Leu117, Val118, His121, Ala122, Ala137, Leu138, Ala140, Pro141, Ile142, Tyr143, Thr144, Phe149
Control		−9.01	Leu83, Ala84	Asn2, Asp3, Asp80, Gly81, Leu82, Tyr113, Pro141, Ile142, Tyr143

tance of 2.2 Å and 2.41 Å, respectively. The terminal 3-ethyl-2,5-dihydrofuran and 3-propyl-2,5-dihydrofuran rings were mostly engaged by van der Waals and alkyl and pi-alkyl interactions. Similarly, the 1-ethyl-1,2,5,5-tetramethyldecahydronaphthalen-4a-ol

and 7-ethyl-2,3-dimethyl-6-oxo-8,9-dihydro-6H-purine-1,3,7-triium of CMNPD8320 were involved in hydrogen bonds with Ala140, Ile142 and Gly81 hydrogen bonds. The entire CMNPD8320 was surrounded by weak hydrophobic contacts. The CMNPD8318

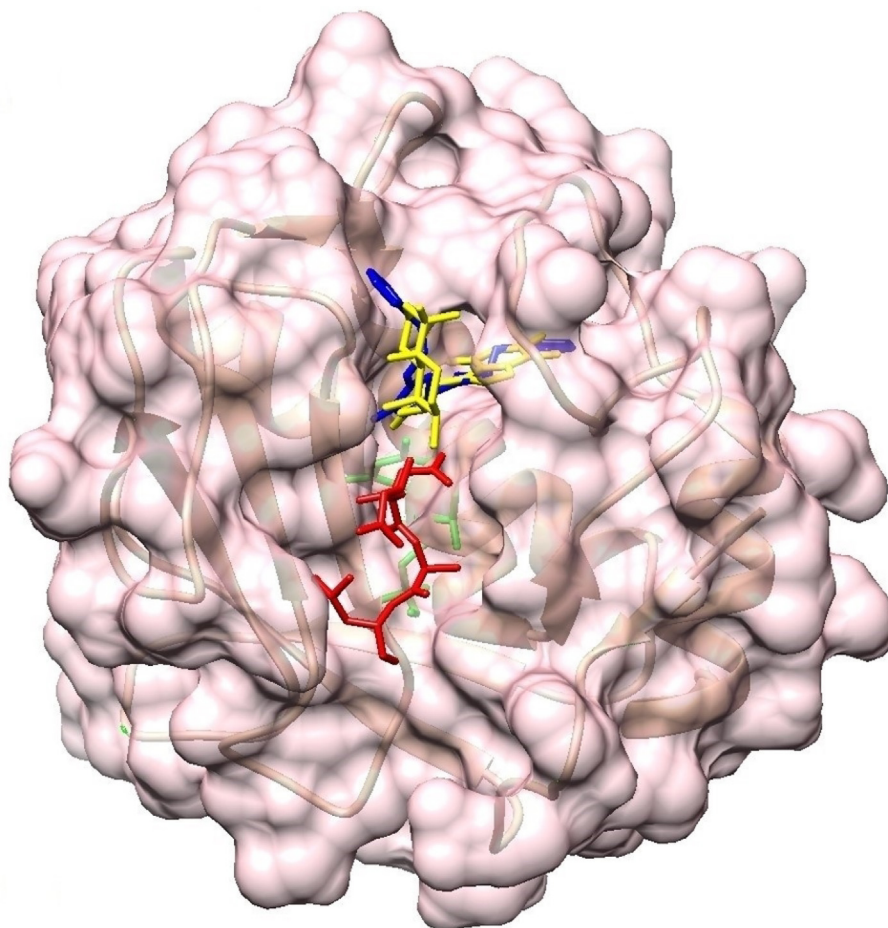


Fig. 2. Docked best binders and control. The MMP-2 catalytic domain is shown by pink surface while docked compounds are presented by different color sticks. The CMNPD8322, CMNPD8320, CMNPD8318 and control are shown by blue, yellow, green and red color.

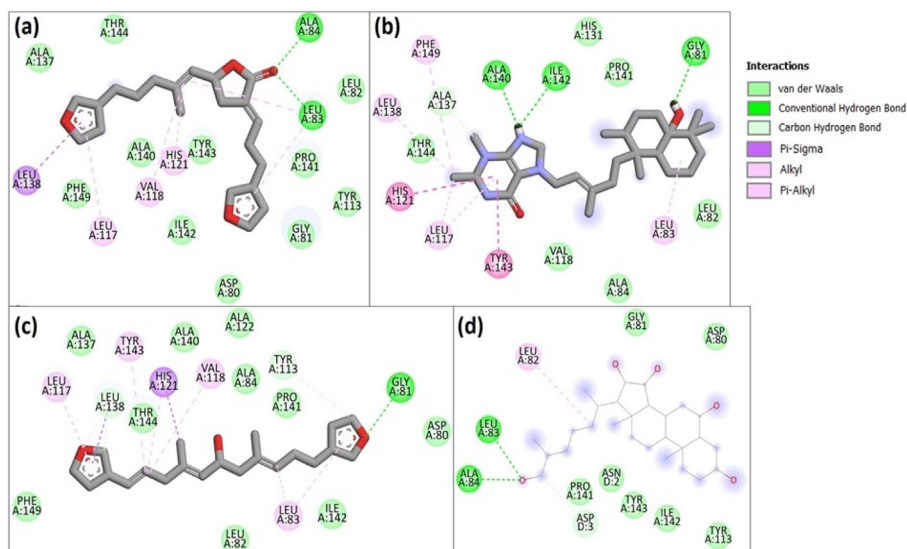


Fig. 3. Intermolecular interactions are provided. (A) CMNPD8322, (b) CMNPD8320, (c) CMNPD8318 and (d) control.

was mostly seen in van der Waals bonding and noticeable interaction was seen with Gly81 at distance of 2.22 Å. All the three lead

structures were seen bonded at the S1 pocket of the MMP-2. The control molecule was also reported to show binding near the S1 pocket with outward structure extension along the active cavity. The good binding energy of the control compound may be due to its key interactions with enzyme active residues. Further, the compound length was seen vital in providing stable conformation along the cavity length. The control molecule produced two strong hydrogen bonds with the enzyme i.e. Ala84 and Leu83. Additionally, the compound reported van der Waals bonding with Asn2, Asp3, Asp80, Gly81, Tyr113, Pro141, Ile142, and Tyr143. The docked compounds conformation is provided in Fig. 2 while the interactions are shown in Fig. 3.

3.2. Molecular dynamic simulations

The molecular dynamic simulation is highly useful approach to study dynamic behavior of docked complexes and decipher real time behavior of docked molecules. This analysis vital to understand the long term of compounds binding to MMP-2 catalytic domain. The first analysis conducted was root mean square deviation (RMSD), followed by root mean square fluctuation (RMSF). Both these analyses were done considering carbon alpha atoms of the MMP-2. The RMSD plots for the systems are shown in

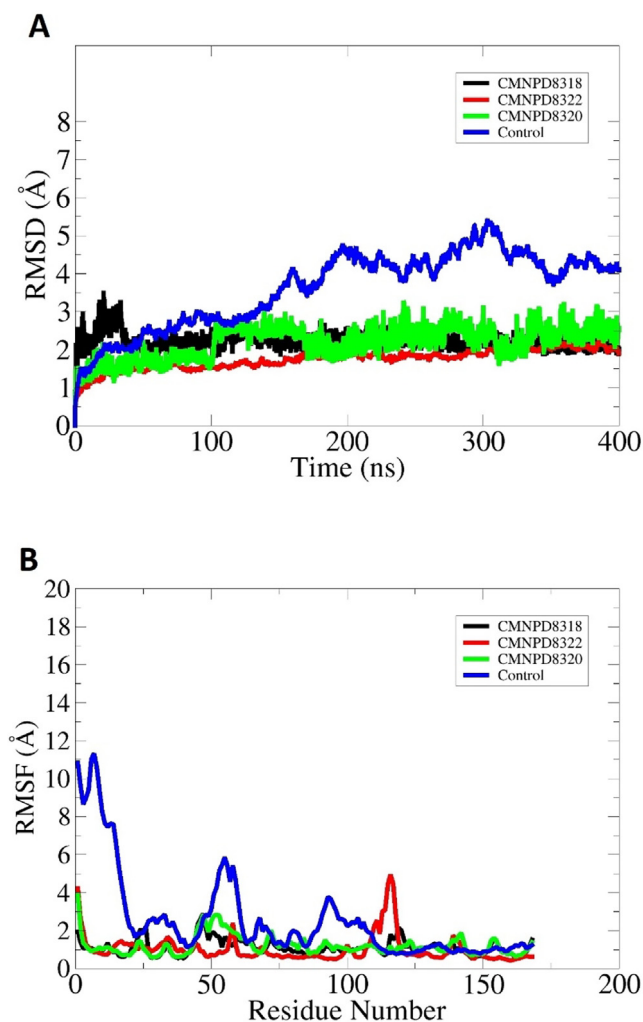


Fig. 4. The dynamic investigation of docked complexes with respect to time (ns). The simulation was done considering the carbon alpha atoms. A. The first assay done was RMSD, followed by RMSF versus MMP-2 residue number (B).

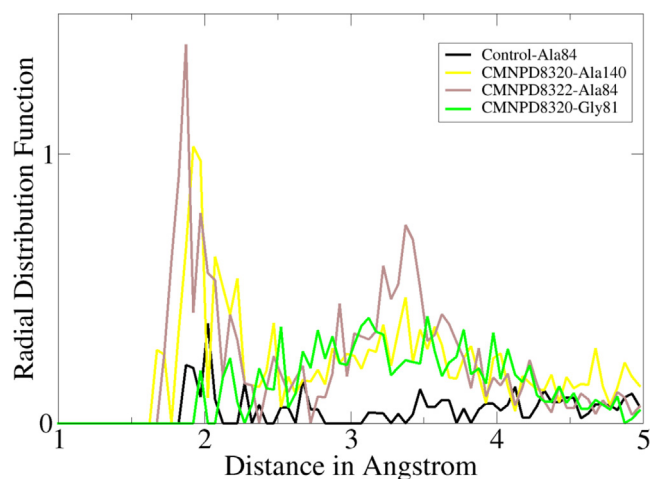


Fig. 5. RDF plots for intermolecular hydrogen bonds between compounds and MMP-2 enzyme.

Table 2

Energy value estimated by different energy term in MM-GB|PBSA analysis.

Energy Term	CMNPD8322	CMNPD8320	CMNPD8318	Control
MM-GBSA				
Van der Waals (kcal/mol)	−46.12	−40.11	−38.39	−35.48
Electrostatic (kcal/mol)	−10.08	−11.65	−10.37	−11.89
Polar (kcal/mol)	10.70	11.36	10.49	9.84
Non-polar (kcal/mol)	−6.19	−6.10	−7.12	−5.11
Gas phase (kcal/mol)	−56.2	−51.76	−48.76	−47.37
Solvation (kcal/mol)	4.51	5.26	3.37	4.73
Delta (kcal/mol)	−51.69	−46.5	−45.39	−42.64
MM-PBSA				
Van der Waals (kcal/mol)	−46.12	−40.11	−38.39	−35.48
Electrostatic (kcal/mol)	−10.08	−11.65	−10.37	−11.89
Polar (kcal/mol)	10.18	9.88	9.69	8.69
Non-polar (kcal/mol)	−7.55	−3.99	−6.51	−6.97
Gas phase (kcal/mol)	−56.2	−51.76	−48.76	−47.37
Solvation (kcal/mol)	2.63	5.89	3.18	1.72
Delta (kcal/mol)	−53.57	−45.87	−45.58	−45.65

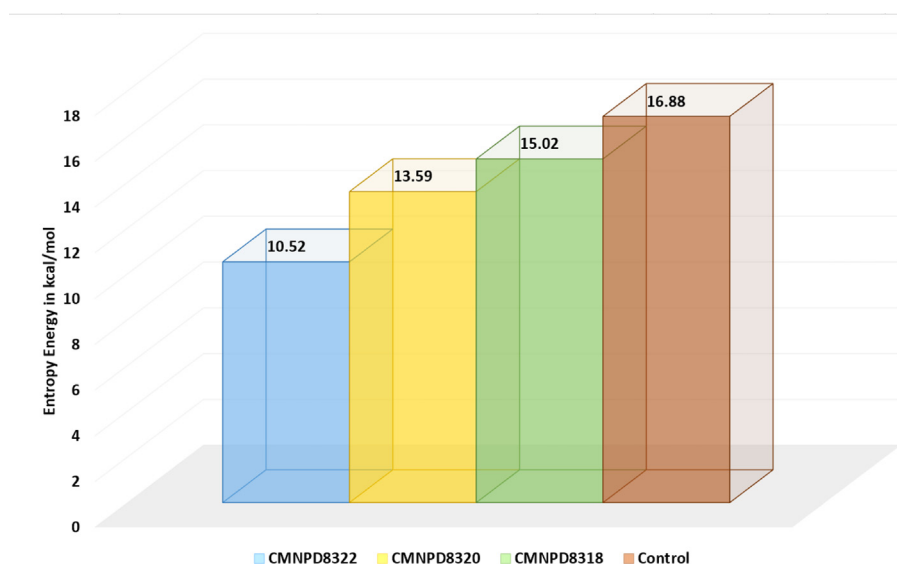
**Fig. 6.** Net entropy energy of compounds and control.

Fig. 4A. The RMSD tells about time dependent structure variations of MMP-2 frames collected at regular time intervals and superimposed over the initial reference structure (Carugo, 2003; Maiorov and Crippen, 1994). It was observed that the control molecule with MMP-2 domain revealed higher RMSD corresponding to higher enzyme structure variations. The control system (shown by blue line) experienced continuous structure changes both in the enzyme as well as in the compound binding conformation as the time proceed. The compounds structure variations were investigated as a mechanism to get a stable binding mode at the docked cavity. The continuous control compound binding mode adjustments forces the MMP-2 enzyme loops to behave more flexibility thus yielding higher RMSD. The maximum RMSD noticed was at 300 ns with RMSD of 5 Å. Towards the simulation end, the control system revealed more stable behavior and reported strong intermolecular interactions and stable docked conformation. Similarly, the CMNPD8322, CMNPD8320, CMNPD8318 systems noticed uniform RMSD dynamics that maximum touches of 2 Å. The CMNPD8318 complex showed a minor RMSD jump up to 4 Å then

experienced very stable plot. The RMSF plots for systems are given in Fig. 4B, which residue wise fluctuations of the simulated complexes (Ahmad et al., 2017). Similarly, like RMSD, the average RMSF of the control complex is higher than prioritized complexes. Three RMSF jumps were noticed for control system. The first jump comprised residues ranges from Met1 to Pro25, while the second and third jumps include residues from Phe40 to Asp60, and Asp80 to Leu107, respectively. Most of these residues lies within the loop regions which are by nature flexible to accommodate conformation changes during catalytic mechanism. Majority residues of the CMNPD8322, CMNPD8320, and CMNPD8318 complexes fall within RMSF value of 2 Å.

3.3. RDF investigation

The intermolecular interactions that were key to docked compounds stability at the enzyme binding site were subjected to RDF analysis that determines interactions density verses distance. The RDF analysis was critical to investigate the maximum inter-

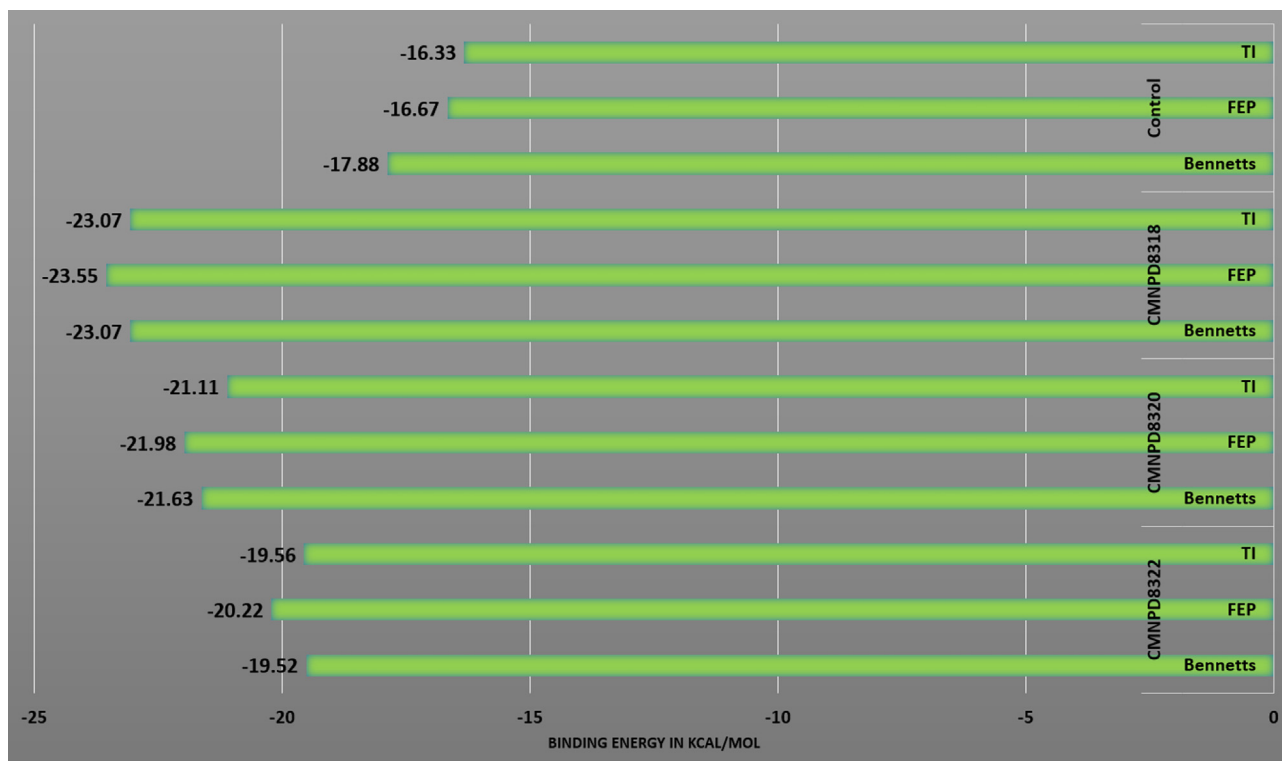


Fig. 7. WaterSwap three algorithms energy value in kcal/mol.

Table 3
ADMET properties investigation of shortlisted compounds.

Property	Compounds			
	CMNPD8322	CMNPD8320	CMNPD8318	Control
Water Solubility	Soluble	Moderately Soluble	Moderately Soluble	Soluble
GI absorption	High	High	High	High
BBB permeant	No	No	Yes	No
Lipinski	Yes	Yes	No	Yes
Veber	Yes	Yes	Yes	Yes
Egan	Yes	Yes	Yes	Yes
Bioavailability Score	0.55	0.55	0.55	0.55
PAINS	0 alert	0 alert	0 alert	1 alert
Synthetic accessibility	4.30	6.55	4.17	5.89
Hepatotoxicity	No	No	No	Yes
Skin Sensitisation	No	No	No	No
AMES toxicity	No	No	No	Yes
Carcino mouse	No	No	No	Yes
Total Clearance	0.310 log ml/min/kg	0.521 log ml/min/kg	0.570 log ml/min/kg	0.714 log ml/min/kg
Renal OCT2 substrate	No	No	No	No

molecular interactions density and their distance. It was observed that CMNPD8322-Ala84 hydrogen bond produced the high interaction density with rdf score of 1.5 and distance of 1.87 Å. Also, the CMNPD8320-Ala140 generate strong hydrogen bond at distance of 1.87 Å. The details of RDF plots for complexes interactions are

given in Fig. 5. Most of the interactions reported in the figure can be seen to have maximum density distribution at very close distance. This suggest that during simulation time, these interactions keep the ligand and interacting enzyme residues at very close distance which in turn make the docked systems stable.

3.4. Estimation of binding energies

The MMPBSA and MMGBSA binding free energies are regarded as powerful tool to validate intermolecular interactions between the lead molecules and receptor. They are considered more appropriate than docking studies as they are based on multiple dynamic snapshots than single docking conformation. The different binding energy terms calculated by MM-GB\PBSA are tabulated in Table 2. According to this analysis, CMNPD8322 was ranked top both in MM-GBSA and MM-PBSA. The net binding energy of CMNPD8322 was -51.69 kcal/mol in MM-GBSA and -53.57 kcal/mol. The CMNPD8320 revealed net energy value of -46.5 kcal/mol (MM-GBSA) and -45.87 kcal/mol (MM-PBSA) whereas value of -45.39 kcal/mol was estimated for CMNPD8318 in MM-GBSA and -45.58 kcal/mol in MM-PBSA. The compounds binding energy reported by MM-GB\PBSA is stable compared to control. The low net binding free energy of control compared to lead molecules in both MM-GBSA and MM-PBSA methods may be due to its unstable binding conformation with the enzyme as noticed in RMSD and RMSF analysis. The continuous changes in the control binding conformation resulted in make/break intermolecular chemical interactions, which in turn causes control compound low binding energy. The van der Waals energy was found as dominating force in making the compound conformation stable at the docked MMP-2 catalytic domain. This was followed by electrostatic energy. The van der Waal energy was favored the most in case of CMNPD8322 where it scored of -46.12 kcal/mol. The control van der Waals contribution was -35.48 kcal/mol. The polar solvation energy was the most non-favorable and contributed the minimum to overall net binding energy.

3.5. Estimation of binding entropy

The estimation of binding entropy for complexes was done separately as this process is computationally expensive. Entropy energy can be define as systems thermal energy that is not available for useful work (Huang et al., 2020). The AMBER normal mode entropy calculation take into account the harmonic frequencies from minimized energy fames of molecular dynamic simulation. The net binding energy of compounds are illustrated in Fig. 6. These net energies were product of three different energies such as translational, rotational and vibrational. Consistent with previous data, the control was the most non-favorable while among the compounds, CMNPD8322 was the least entropy free energy contributor. This demonstrate that the compound is the most stable among the lead molecules and control.

3.6. Calculation of WaterSwap energies

The WaterSwap energies were calculated as to get additional confirmation on the intermolecular docked stability of complexes. The water molecules role that bridge the compounds with MMP-2 protein active site residues were taken into account. The WaterSwap reported three algorithms binding energy; FEP, TI and Bennett's (Fig. 7). According to WaterSwap, the CMNPD8318 is the most promising lead, followed by CMNPD8320. The CMNPD8318 FEP, TI and Bennett's binding energy value is -23.55 kcal/mol, -23.07 kcal/mol and -23.07 kcal/mol, respectively. The CMNPD8320 energy value for FEP is -21.98 kcal/mol, TI is -21.11 kcal/mol and Bennett's is -21.63 kcal/mol. The control net binding energy value is -16.33 kcal/mol for TI, -16.67 kcal/mol for FEP, and -17.88 kcal/mol for Bennett's. The energy values of complexes are not different by 1 kcal/mol which demonstrates well convergence of the WaterSwap analysis.

3.7. Pharmacokinetic analysis of lead molecules

The different pharmacokinetic analyses of lead molecules were determined in order to shed light whether the compounds will be suitable structures from absorption, distribution, metabolism, excretion, and toxicity (ADMET) perspective (Van De Waterbeemd and Gifford, 2003). The compounds were reported to have good water solubility and thus can be reached in higher concentration to the target site (Bergström and Larsson, 2018). This was also supported by high gastrointestinal absorption of the compounds thus concluding high amount of the molecules at the target site for maximum therapeutic effect (Zhang and Benet, 2001). The compounds are also classified as good druglike molecules as they fulfill all parameters of the Lipinski rule of five, Veber and Egan drug rules. All the three compounds showed no alert for Pan-assay interference compounds (PAINS) which revealed that the compounds showed interactions with only one biological target and does not give false positive results (Whitty, 2011). The compounds are also non-mutagenic and non-toxic thus have less chances to discarded in further trails studies. In contrast the control molecule, despite being a good druglike candidate by following all the major druglike rule yet it has one alert for PAINS, and is toxic as per hepatotoxicity, carcino mouse, and AMES toxicity test. Details of the compounds ADMET properties are given in Table 3.

4. Conclusions

In this work, three drug molecules: CMNPD8322, CMNPD8320, and CMNPD8318 were surface that binding best to the catalytic domain of MMP-2 enzyme, which is a promising anti-cancer target. The binding conformation of the said compounds to enzyme was determined very stable throughout the simulation time and inter-molecular interaction energies especially van der Waals and electrostatic were the dominating factors. The compounds were disclosed to show favorable pharmacokinetic properties and have good oral bioavailability score. Similarly, the compounds were revealed not to contain toxic chemical moieties and are non-mutagenic. Altogether, the compounds prioritized in this study can be utilized in experimental studies to determine whether they can show actual biological MMP-2 enzyme inhibition.

Declaration of Competing Interest

The authors declare that they have no known competing financial interests or personal relationships that could have appeared to influence the work reported in this paper.

References

- Abbasi, S., Raza, S., Azam, S.S., Liedl, K.R., Fuchs, J.E., 2016. Interaction mechanisms of a melatonergic inhibitor in the melatonin synthesis pathway. *J. Mol. Liq.* 221, 507–517.
- Abro, A., Azam, S.S., 2016. Binding free energy based analysis of arsenic (+ 3 oxidation state) methyltransferase with S-adenosylmethionine. *J. Mol. Liq.* 220, 375–382.
- Ahmad, S., Raza, S., Uddin, R., Azam, S.S., 2017. Binding mode analysis, dynamic simulation and binding free energy calculations of the MurF ligase from *Acinetobacter baumannii*. *J. Mol. Graph. Model.* 77, 72–85. <https://doi.org/10.1016/j.jmkgm.2017.07.024>.
- Ahmad, S., Raza, S., Uddin, R., Azam, S.S., 2018. Comparative subtractive proteomics based ranking for antibiotic targets against the dirtiest superbug: *Acinetobacter baumannii*. *J. Mol. Graph. Model.* 82, 74–92. <https://doi.org/10.1016/j.jmkgm.2018.04.005>.
- Ahmad, S., Ranaghan, K.E., Azam, S.S., 2019a. Combating tigecycline resistant *Acinetobacter baumannii*: A leap forward towards multi-epitope based vaccine discovery. *Eur. J. Pharm. Sci.* 132, 1–17.
- Ahmad, S., Raza, S., Abro, A., Liedl, K.R., Azam, S.S., 2019b. Toward novel inhibitors against KdsB: a highly specific and selective broad-spectrum bacterial enzyme. *J. Biomol. Struct. Dyn.* 37, 1326–1345.

- Ahmad, S., Waheed, Y., Ismail, S., Abbasi, S.W., Najmi, M.H., 2021. A computational study to disclose potential drugs and vaccine ensemble for COVID-19 conundrum. *J. Mol. Liq.* 324, 114734.
- Alamri, M.A., Tariq, M.H., Tahir ul Qamar, M., Alabbas, A.B., Alqahtani, S.M., Ahmad, S., 2023. Discovery of potential phytochemicals as inhibitors of TcdB, a major virulence factors of Clostridioides difficile. *J. Biomol. Struct. Dyn.*, 1–9.
- Altharawi, A., Ahmad, S., Alamri, M.A., ul Qamar, M.T., 2021. Structural insight into the binding pattern and interaction mechanism of chemotherapeutic agents with Sorcin by docking and molecular dynamic simulation. *Colloids Surf. B Biointerfaces* 112098.
- Banerjee, S., Lo, W.-C., Majumder, P., Roy, D., Ghorai, M., Shaikh, N.K., Kant, N., Shekhawat, M.S., Gaddekar, V.S., Ghosh, S., et al., 2022. Multiple roles for basement membrane proteins in cancer progression and EMT. *Eur. J. Cell Biol.* 151220.
- Barve, A., Jin, W., Cheng, K., 2014. Prostate cancer relevant antigens and enzymes for targeted drug delivery. *J. Control. Release* 187, 118–132.
- Benton, G., Kleinman, H.K., George, J., Arnaoutova, I., 2011. Multiple uses of basement membrane-like matrix (BME/Matrigel) in vitro and in vivo with cancer cells. *Int. J. Cancer* 128, 1751–1757.
- Bergström, C.A.S., Larsson, P., 2018. Computational prediction of drug solubility in water-based systems: qualitative and quantitative approaches used in the current drug discovery and development setting. *Int. J. Pharm.* 540, 185–193.
- Biovia, D.S., 2017. Discovery studio visualizer. San Diego, CA, USA.
- Bodnar, M., Szyllberg, Ł., Kazmierczak, W., Marszałek, A., 2015. Tumor progression driven by pathways activating matrix metalloproteinases and their inhibitors. *J. Oral Pathol. Med.* 44, 437–443.
- Brown, G.T., Murray, G.I., 2015. Current mechanistic insights into the roles of matrix metalloproteinases in tumour invasion and metastasis. *J. Pathol.* 237, 273–281.
- Carugo, O., 2003. How root-mean-square distance (rmsd) values depend on the resolution of protein structures that are compared. *J. Appl. Cryst.* 36, 125–128.
- Case, D.A., Belfon, K., Ben-Shalom, I., Brozell, S.R., Cerutti, D., Cheatham, T., Cruzeiro, V.W.D., Darden, T., Duke, R.E., Giambasu, G., others, 2020. Amber 2020.
- Daina, A., Michielin, O., Zoete, V., 2017. SwissADME: A free web tool to evaluate pharmacokinetics, drug-likeness and medicinal chemistry friendliness of small molecules. *Sci. Rep.* 7, 1–13. <https://doi.org/10.1038/srep42717>.
- Dallakyan, S., Olson, A.J., 2015. Small-molecule library screening by docking with PyRx. *Springer*, pp. 243–250.
- Donohue, J., 1954. Radial Distribution Functions of Some Structures of the Polypeptide Chain. *Proc. Natl. Acad. Sci.* 40, 377–381. <https://doi.org/10.1073/pnas.40.6.377>.
- Dvorak, H.F., Weaver, V.M., Tlsty, T.D., Bergers, G., 2011. Tumor microenvironment and progression. *J. Surg. Oncol.* 103, 468–474.
- Genheden, S., Kuhn, O., Mikulskis, P., Hoffmann, D., Ryde, U., 2012. The normal-mode entropy in the MM/GBSA method: effect of system truncation, buffer region, and dielectric constant. *J. Chem. Inf. Model.* 52, 2079–2088.
- Hassan Baig, M., Ahmad, K., Roy, S., Mohammad Ashraf, J., Adil, M., Haris Siddiqui, M., Khan, S., Amjad Kamal, M., Provaznik, I., Choi, I., 2016. Computer aided drug design: success and limitations. *Curr. Pharm. Des.* 22, 572–581.
- Hernandez-Guillamon, M., Mawhirt, S., Blais, S., Montaner, J., Neubert, T.A., Rostagno, A., Ghiso, J., 2015. Sequential amyloid- β degradation by the matrix metalloproteinases MMP-2 and MMP-9. *J. Biol. Chem.* 290, 15078–15091.
- Huang, K., Luo, S., Cong, Y., Zhong, S., Zhang, J.Z.H., Duan, L., 2020. An accurate free energy estimator: based on MM/PBSA combined with interaction entropy for protein–ligand binding affinity. *Nanoscale* 12, 10737–10750.
- Hung, S.-Y., Lin, C.-Y., Yu, C.-C., Chen, H.-T., Lien, M.-Y., Huang, Y.-W., Fong, Y.-C., Liu, J.-F., Wang, S.-W., Chen, W.-C., et al., 2021. Visfatin promotes the metastatic potential of chondrosarcoma cells by stimulating ap-1-dependent mmp-2 production in the mapk pathway. *Int. J. Mol. Sci.* 22, 8642.
- Jezierska, A., Motyl, T., 2009. Matrix metalloproteinase-2 involvement in breast cancer progression: a mini-review. *Med. Sci. Monitor: Int. Med. J. Exp. Clin. Res.* 15, RA32–40.
- Kaliappan, S., Bombay, I.I.T., 2018. UCSF Chimera-Overview.
- Kessenbrock, K., Plaks, V., Werb, Z., 2010. Matrix metalloproteinases: regulators of the tumor microenvironment. *Cell* 141, 52–67.
- Khan, M.M., Filipczak, N., Torchilin, V.P., 2021. Cell penetrating peptides: A versatile vector for co-delivery of drug and genes in cancer. *J. Control. Release* 330, 1220–1228.
- Kräutler, V., Van Gunsteren, W.F., Hünenberger, P.H., 2001. A fast SHAKE algorithm to solve distance constraint equations for small molecules in molecular dynamics simulations. *J. Comput. Chem.* 22, 501–508.
- Kurzepa, J., Kurzepa, J., Golab, P., Czerska, S., Bielewicz, J., 2014. The significance of matrix metalloproteinase (MMP)-2 and MMP-9 in the ischemic stroke. *Int. J. Neurosci.* 124, 707–716.
- L Mallipeddi, P., Kumar, G., W White, S., R Webb, T., 2014. Recent advances in computer-aided drug design as applied to anti-influenza drug discovery. *Curr. Top. Med. Chem.* 14, 1875–1889.
- Lipinski, C.A., 2004. Lead- and drug-like compounds: The rule-of-five revolution. *Drug Discov. Today Technol.* 1, 337–341. <https://doi.org/10.1016/j.ddtec.2004.11.007>.
- Lombardo, F., Desai, P.V., Arimoto, R., Desino, K.E., Fischer, H., Keefer, C.E., Petersson, C., Winawater, S., Broccatelli, F., 2017. In Silico Absorption, Distribution, Metabolism, Excretion, and Pharmacokinetics (ADME-PK): Utility and Best Practices. An Industry Perspective from the International Consortium for Innovation through Quality in Pharmaceutical Development: Miniperspective. *J. Med. Chem.* 60, 9097–9113.
- Lyu, C., Chen, T., Qiang, B., Liu, N., Wang, H., Zhang, L., Liu, Z., 2021. CMNPD: a comprehensive marine natural products database towards facilitating drug discovery from the ocean. *Nucleic Acids Res.* 49, D509–D515.
- Maia, E.H.B., Assis, L.C., de Oliveira, T.A., da Silva, A.M., Taranto, A.G., 2020. Structure-based virtual screening: From classical to artificial intelligence. *Front. Chem.* 8.
- Maier, J.A., Martinez, C., Kasavajhala, K., Wickstrom, L., Hauser, K.E., Simmerling, C., 2015. ff14SB: improving the accuracy of protein side chain and backbone parameters from ff99SB. *J. Chem. Theory Comput.* 11, 3696–3713.
- Maierov, V.N., Crippen, G.M., 1994. Significance of root-mean-square deviation in comparing three-dimensional structures of globular proteins.
- Miller, B.R., McGee, T.D., Swails, J.M., Homeyer, N., Gohlke, H., Roitberg, A.E., 2012. MMPBSA.py: An efficient program for end-state free energy calculations. *J. Chem. Theory Comput.* 8, 3314–3321. <https://doi.org/10.1021/ct300418h>.
- Muhseen, Z.T., Hameed, A.R., Al-Hasani, H.M.H.H., ul Qamar, M.T., Li, G., Tahir ul Qamar, M., Li, G., 2020. Promising terpenes as SARS-CoV-2 spike receptor-binding domain (RBD) attachment inhibitors to the human ACE2 receptor: integrated computational approach. *J. Mol. Liq.* 320, 114493. <https://doi.org/10.1016/j.molliq.2020.114493>.
- Noor, F., Ashfaq, U., Bakar, A., Tahir Ul Qamar, M., n.d. Discovering common pathogenic processes between COVID-19 and HFRS by integrating RNA-Seq differential expression analysis with machine learning. *Front. Microbiol.* 14, 1188.
- Petersen, H.G., 1995. Accuracy and efficiency of the particle mesh Ewald method. *J. Chem. Phys.* 103, 3668–3679.
- Pires, D.E.V., Blundell, T.L., Ascher, D.B., 2015. pkCSM: Predicting small-molecule pharmacokinetic and toxicity properties using graph-based signatures. *J. Med. Chem.* 58, 4066–4072. <https://doi.org/10.1021/acs.jmedchem.5b00104>.
- Roe, D.R., Cheatham III, T.E., 2013. PTRAJ and CPPTRAJ: software for processing and analysis of molecular dynamics trajectory data. *J. Chem. Theory Comput.* 9, 3084–3095.
- Sahakyan, H., 2021. Improving virtual screening results with MM/GBSA and MM/PBSA rescoring. *J. Comput. Aided Mol. Des.* 35, 731–736.
- Shaker, B., Ahmad, S., Lee, J., Jung, C., Na, D., 2021. In silico methods and tools for drug discovery. *Comput. Biol. Med.* 104851.
- Singh, A., Vanga, S.K., Orsat, V., Raghavan, V., 2018. Application of molecular dynamic simulation to study food proteins: A review. *Crit. Rev. Food Sci. Nutr.* 58, 2779–2789.
- Sprenger, K.G., Jaeger, V.W., Pfandtner, J., 2015. The general AMBER force field (GAFF) can accurately predict thermodynamic and transport properties of many ionic liquids. *J. Phys. Chem. B* 119, 5882–5895.
- Sussman, J.L., Lin, D., Jiang, J., Manning, N.O., Prilusky, J., Ritter, O., Abola, E.E., 1998. Protein Data Bank (PDB): database of three-dimensional structural information of biological macromolecules. *Acta Crystallogr. D Biol. Crystallogr.* 54, 1078–1084.
- Tahir ul Qamar, M., Alqahtani, S.M., Alamri, M.A., Chen, L.-L.L., ul Qamar, M.T., Alqahtani, S.M., Alamri, M.A., Chen, L.-L.L., 2020. Structural basis of SARS-CoV-2 3CLpro and anti-COVID-19 drug discovery from medicinal plants. *J. Pharm. Anal.* 10, 313–319. <https://doi.org/10.1016/j.jpha.2020.03.009>.
- Takeuchi, T., Hayashi, M., Tamita, T., Nomura, Y., Kojima, N., Mitani, A., Takeda, T., Hitaka, K., Kato, Y., Kamitani, M., et al., 2022. Discovery of Aryloxyphenyl-Heptapeptide Hybrids as Potent and Selective Matrix Metalloproteinase-2 Inhibitors for the Treatment of Idiopathic Pulmonary Fibrosis. *J. Med. Chem.*
- Tauro, M., Lynch, C.C., 2018. Cutting to the chase: how matrix metalloproteinase-2 activity controls breast-cancer-to-bone metastasis. *Cancers* 10, 185.
- Turner, P.J., 2005. XMGRACE, Version 5.1. 19. Center for Coastal and Land-Margin Research. Oregon Graduate Institute of Science and Technology, Beaverton, OR.
- Ullah, A., Ahmad, S., Ismail, S., Afsheen, Z., Khurram, M., Tahir ul Qamar, M., AlSuhaymi, N., Alsugoor, M.H., Allemaillem, K.S., 2021. Towards A Novel Multi-Epitopes Chimeric Vaccine for Stimulating Strong Immune Responses and Protection against *Morganella morganii*. *Int. J. Environ. Res. Public Health* 18, 10961.
- Van De Waterbeemd, H., Gifford, E., 2003. ADMET in silico modelling: towards prediction paradise? *Nat. Rev. Drug Discov.* 2, 192–204.
- Vandenbroucke, R.E., Libert, C., 2014. Is there new hope for therapeutic matrix metalloproteinase inhibition? *Nat. Rev. Drug Discov.* 13, 904–927.
- Vandooren, J., Opendakker, G., Loadman, P.M., Edwards, D.R., 2016. Proteases in cancer drug delivery. *Adv. Drug Deliv. Rev.* 97, 144–155.
- Wang, E., Sun, H., Wang, J., Wang, Z., Liu, H., Zhang, J.Z.H., Hou, T., 2019. End-point binding free energy calculation with MM/PBSA and MM/GBSA: strategies and applications in drug design. *Chem. Rev.* 119, 9478–9508.
- Webb, A.H., Gao, B.T., Goldsmith, Z.K., Irvine, A.S., Saleh, N., Lee, R.P., Lendermon, J.B., Bheemreddy, R., Zhang, Q., Brennan, R.C., et al., 2017. Inhibition of MMP-2 and MMP-9 decreases cellular migration, and angiogenesis in in vitro models of retinoblastoma. *BMC Cancer* 17, 1–11.
- Whitty, A., 2011. Growing PAINS in academic drug discovery. *Future Med. Chem.* 3, 797–801.
- Winer, A., Adams, S., Mignatti, P., 2018. Matrix metalloproteinase inhibitors in cancer therapy: turning past failures into future successes. *Mol. Cancer Ther.* 17, 1147–1155.

- Wolber, G., Langer, T., 2005. LigandScout: 3-D pharmacophores derived from protein-bound ligands and their use as virtual screening filters. *J. Chem. Inf. Model.* 45, 160–169. <https://doi.org/10.1021/ci049885e>.
- Woods, C.J., Malaisree, M., Hannongbua, S., Mulholland, A.J., 2011. A water-swap reaction coordinate for the calculation of absolute protein-ligand binding free energies. *J. Chem. Phys.* 134. <https://doi.org/10.1063/1.3519057>.
- Woods, C.J., Malaisree, M., Michel, J., Long, B., McIntosh-Smith, S., Mulholland, A.J., 2014. Rapid decomposition and visualisation of protein-ligand binding free energies by residue and by water. *Faraday Discuss* 169, 477–499. <https://doi.org/10.1039/c3fd00125c>.
- Zhang, Y., Benet, L.Z., 2001. The gut as a barrier to drug absorption. *Clin. Pharmacokinet.* 40, 159–168.
- Zhong, Y., Lu, Y.-T., Sun, Y., Shi, Z.-H., Li, N.-G., Tang, Y.-P., Duan, J.-A., 2018. Recent opportunities in matrix metalloproteinase inhibitor drug design for cancer. *Expert Opin. Drug Discov.* 13, 75–87.